12th International Conference on Fracture Mechanics of Concrete and Concrete Structures
FraMCoS-12
B.L.A. Pichler, Ch. Hellmich, P. Preinstorfer (Eds)

https://doi.org/10.21012/FC12.1346
MS11:2

COUPLED REACTIVE TRANSPORT AND POROMECHANICS MODELLING OF EXTERNAL SULFATE ATTACK IN CEMENTITIOUS MATERIALS

SYED YASIR ALAM[*], ANTHONY SOIVE[†] AND AHMED LOUKILI[*]

[*] Nantes Université, Ecole Centrale de Nantes, CNRS, GeM UMR 6183, F-44000 Nantes, France
e-mail: syed-yasir.alam@ec-nantes.fr, ahmed.loukili@ec-nantes.fr, www.ec-nantes.fr

[†] Cerema Méditerranée, Aix-en-Provence, France
e-mail: anthony.soive@cerema.fr, www.cerema.fr

Key words: external sulfate attack, chemo-mechanics, micromechanics, C-S-H, crystallisation pressure

Abstract: External sulfate attack (ESA) is a leading cause of durability deterioration in concrete structures, primarily driven by expansion due to crystallization pressures associated with ettringite formation. This research develops a novel chemo-mechanical model to simulate degradation in cementitious materials under ESA conditions. The model integrates a pore-scale representation of the C-S-H gel, considering both reactive transport and poromechanical effects. Chemically, the model incorporates precipitation/dissolution kinetics and ionic adsorption/desorption at the C-S-H phase within a comprehensive reactive transport framework. Mechanically, a poromechanical model is coupled to the transport processes to capture local strain effects at the C-S-H gel scale. Three primary mechanisms contribute to the mechanical response: (i) the chemical reaction between monosulfate within the C-S-H phase and incoming sulfate ions, resulting in the eventual consumption of monosulfates, (ii) sulfate adsorption and subsequent desorption from the C-S-H surface, resulting in ettringite precipitation, and (iii) crystallization pressure exerted within the gel's interstitial porosity, driven by the equilibrium of sulfate ions in solution. The fully coupled chemo-mechanical model provides robust predictions of sulfate ion transport, capturing both the spatial and temporal evolution of sulfate adsorption in the C-S-H phase, while identifying zones with high sulfate concentrations. Additionally, the model reveals the influence of material parameters on chemo-mechanical interactions, offering valuable insights into their role in controlling mechanical expansion. The results show an encouraging correlation between predicted and experimental macroscopic strain values, validating the model's ability to simulate sulfate-induced degradation mechanisms in cementitious systems.

1 INTRODUCTION

Underground and offshore structures can be in contact with water, which contains sulfates affecting the durability of cementitious materials used in these structures. Sulfate propagates into the material and modifies transport and mechanical properties, which is known as External Sulfate Attacks (ESA). Indeed, even after the complete hydration of cement paste, the interstitial solution of mortar or concrete is actually in a metastable thermodynamic equilibrium with various solid phases. The ingress of external sulfate changes the chemical composition of the interstitial solution and disturbs the local thermodynamic equilibrium and the pH, which leads to dissolution and precipitation. Depending upon chemical interaction of a sulfate rich water with the cement paste, the pH of the interstitial

solution falls due to penetration of aggressive solutions containing sulfates, leading to calcium leaching including dissolution of the CH and decalcification of the C-S-H. The calcium and sulfate ions can react with mono-sulfate to form ettringite that is so expansive and will lead to formation of cracks affecting the durability of material.

The modelling of expansion due to ESA can be assumed as a chemo mechanical coupled problem. Tixier and Mobasher [1] assumed the volumetric expansion as an eigenstrain. Basista and Weglewski [2] used a micromechanical approach to determine the eigenstrain developed by ettringite formation in cement paste. Bary 2008 [3] and Bary et al. 2014 [4] assumed the expansion is caused by the crystallization pressure, generated by growing of small AFm crystals embedded in C–S–H matrix and by the precipitation of ettringite in small pores (Schmidt et al. [5] and Yu et al. [6]). More recently, Gu et al. proposes an advanced model of the expansion of cementitious materials based on interface-controlled crystal growth mechanisms (Gu et al. [7]). However, in all these models, the influence of sulfates adsorbed on C-S-H is not considered. The purpose of this research is to quantify this role.

In this paper, an improved chemo-mechanical coupled model is presented which considers several mechanisms in the first's steps of the deformation of the material. The ingress of sulfate is modelled by physically and chemically coupled model taking into account multi-ionic diffusion, precipitation/dissolution kinetics and surface complexation (Soive et al. [8]). A new model is proposed for ettringite precipitation in the interstitial gel porosity of C-S-H gel structure based on chemical equilibrium of sulfate ions in the solution. Further, the expansion is assumed to occur by expansion of gel pores without cracks as the mechanical behaviour is considered as elastic during the first's days of exposure. The mechanical model used is the C-S-H level poromechanical model (Rhardane et al. [9]) founded on the mechanism of crystallization pressure, which is believed to be the driving force responsible for expansion of cementitious materials.

2 C-S-H PORE MODEL

The interaction between the sulfate ions and C-S-H lead to many mechanisms: dissolution/precipitations mechanisms, adsorption/desorption of sulfates ions on C-S-H surface that depend on the equilibrium between pore solution and surface of C-S-H but also the concentration of sulfate ions incoming to pore of C-S-H by diffusion mechanism like it is shown in the Figure 1.

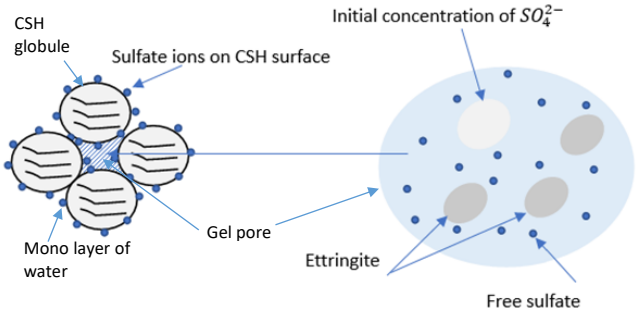

Figure 1: Illustration of different mechanisms in the level of C-S-H gel.

In this study, the concentration of free ions in the gel pore is defined from the different concentration produced or consumed by different mechanisms in the C-S-H level. The concentration of sulphate ions given by the dissolution of monosulphate ($C_{disso,CSH}$) and ions desorbed from the C-S-H surface ΔC in addition to the sulphate ions given by diffusion ($C_{Diff,CSH}$) will precipitate as ettringite in the gel pore. The summation of these concentrations in every time step gives the concentration of free sulphate ion $C_{free,CSH}(t_{i+1})$ as follows:

$$C_{free,CSH}(t_{i+1}) = C_{in,CSH}(t_i) + C_{Diff,CSH}(t_{i+1}) - \Delta C(t_{i+1}) + C_{disso,CSH}(t_{i+1}) \quad (1)$$

Adsorption/Desorption mechanisms

The concentration of sulfate ions adsorbed or desorbed by C-S-H at time t for different depth can be determined by the reactive transport model (Soive et al. [8]). The variation can then be calculated as follows:

$$\Delta C(t_{i+1}) = C_{ads,CSH}(t_{i+1}) - C_{ads,CSH}(t_i) \quad (2)$$

If:

$\Delta C(t_{i+1}) > 0$: donate the concentration of sulfate ions adsorbed in $(t_{i+1} - t_i)$

$\Delta C(t_{i+1}) < 0$: donate the concentration of sulfate ions desorbed in $(t_{i+1} - t_i)$.

2.2 Precipitation mechanism

To calculate the concentration of sulfate ions precipitated as ettringite $C_{preci,CSH}(t_{i+1})$, kinetic law given by Soive et al. [8] can be used with $C_{free,CSH}(t_{i+1})$ as input.
We will define also $C_{in,CSH}(t_i)$ as molar concentration of sulfate ions at the previous instant t_i that will be initialized in every step of calculation.

$$C_{in,CSH}(t_{i+1}) = C_{free,CSH}(t_{i+1}) - C_{preci,CSH}(t_{i+1}) \quad (3)$$

The kinetic law is defined as the kinetic rate of ettringite formation as follows:

$$r_n = f(C_1, C_2, \dots, C_{N_c}) = \pm k_n A_{ms,n} |1 - \Omega_n^{\theta}|^{\eta} \quad (4)$$

where:
$n = 1, \dots, N_q$
k_n is the rate constant (moles per unit mineral surface area and unit time)
$A_{ms,n}$ is the specific reactive surface area per kg H_2O

$$A_{ms,n} = (V_{frac}\, A_m) / C_w \quad (5)$$

V_{frac} is the mineral volume fraction in units of m^3 mineral/m^3 medium, A_m is the surface area of minerals in units of m^2 mineral/m^3 mineral and C_w is the wetted-surface conversion factor in units of kg water/m^3 medium.
Ω_n^{θ} is the saturation index.
To define the concentration of ettringite precipitated as function of time and chemical activities of ions, the above equations become:

$$\frac{dC_{ett}}{dt} = K_{ett} A_{ms,ett} |1 - \Omega_{ett}| \quad (6)$$

$$C_{ett,CSH}(t_{i+1}) = C_{ett,CSH}(t_i) + K_{ett} A_{ms,ett} \Delta t |1 - \Omega_{ett}| \quad (7)$$

with:

$$\Omega_{ett} = \frac{Q_{ett}}{K_{eq,ett}} \quad (8)$$

$$Q_{ett} = (\gamma_{Ca^{2+}} C_{Ca^{2+}})^6 \times \left(\gamma_{SO_4^{2-}} C_{free,CSH}\right)^3 \times (\gamma_{Al^{3+}} C_{Al^{3+}})^2 \times (\gamma_{OH^-} C_{OH^-})^{12} \quad (9)$$

where C_{ett} and Ω_{ett} designate the concentration and the saturation index (or formation index) of ettringite, respectively, and K_{ett} [mol. m^{-2} s^{-1}] is a kinetics coefficient.
$K_{eq,ett}$ is the equilibrium constant of ettringite ($\log(K_{eq,ett}) = -45.09$ (from Lothenbach and Winnefeld [10])

2.3 Dissolution of monosulfate

According to Bary et al. [4], the main reaction in ESA is:

$$3CaOAl_2O_3CaSO_4 12H_2O + 2Ca^{2+} + 2SO_4^{2-} + 20H_2O \Longleftrightarrow 3CaOAl_2O_3 3CaSO_4 32H_2O \quad (10)$$

The equation shows that the precipitation of ettringite (Aft) is the result of the dissolution of monosulfate (AFm) in the presence of sulfate ions. Thus, the reaction of dissolution of AFm can be written as follows:

$$3CaOAl_2O_3CaSO_4 12H_2O(s) \Longleftrightarrow 4Ca^{2+} + 2Al(OH)_4{}^- + SO_4^{2-} + 4OH^- + 6H_2O \quad (11)$$

In order to calculate the concentration of ettringite in the pore gel, the concentration of different ions in the pore gel: SO_4^{2-}, Ca^{2+}, $Al(OH)_4^-$ and OH^- (which are the results of dissolution of monosulfate, as shown in the last equation) should be known. However, the concentration of AFm phase is not known, since its distribution in the mortar specimen is not homogeneous. Yu et al. [6] precised that most of these AFm phases are finely intermixed with the C–S–H phase even if we do not know precisely how it is distributed. In order to calculate the amount of AFm embedded in C-S-H gel, we define a coefficient α_{AFm} as follows:

$$C_{AFm,CSH} = \alpha_{AFm} \times C_{AFm,spec} \quad (12)$$

$C_{AFm,CSH}$: Molar concentration of AFm phase in C-S-H gel

$C_{AFm,spec}$: Molar concentration of AFm phase in specimen

The concentration of AFm in the specimen at different time output can be obtained from the reactive transport model. In order to calculate the concentration of AFm phase embedded in the C-S-H gel, calculations are performed for different values of α_{AFm}, with an initial value of 0.6. Further, the dissolution of AFm phase ($3CaOAl_20_3CaSO_412H_2O$) gives the concentration of different ions ${SO_4}^{2-}$, ${Ca}^{2+}$, ${Al}^{3+}$ and ${OH}^{-}$ as follows:

$C_{Ca^{2+}} = 4 \times \mathrm{C}_{\mathrm{AFm,CSH}}$

$C_{SO_4^{2-}} = \mathrm{C}_{\mathrm{AFm,CSH}}$

$C_{\ Al^{3+}} = 2 \times \mathrm{C}_{\mathrm{AFm,CSH}}$

$C_{OH^-} = 4 \times \mathrm{C}_{\mathrm{AFm,CSH}}$

2.4 Diffusion of sulfate ions

In most experimental studies, the specimen is immersed in a solution containing sulfate ions to simulate the effect of ingress of sulfate ions into the specimen and the mean mechanism of this phenomena can be attributed as the diffusion of sulfate ions in the material. A major part of sulfate ions diffused in the material react during different mechanisms: dissolution/precipitation, complexation on surface… and minor part will be free in the interstitial solution. In this study, since we are focusing our research at the C-S-H level, by using reactive transport model, we can determine the concentration $C_{Diff,CSH}(t_{i+1})$ in the pore gel at every time output that will not react so will be free in the interstitial solution. However, this quantity is negligible.

3 POROMECHANICAL MODEL

This section presents the formulation of the micromechanical model for external sulfate attack phenomena in cementitious materials. In fact, the leaching of portlandite and ettringite crystallization pressure cause an increase of porosity, expansion, cracking and consequently a loss of mechanical property and an increase in permeability. This model also takes into account the pore size distribution, the saturation of ettringite as function of pore radius, the saturation as function of time and chemical kinetics, the crystallization pressure, and the deformation as a function of time.

3.1 Pore size distribution

The normalized cumulated pore volume based on the Brunauer-Skalny-Bodor (BSB) adsorption model that depend on the relative humidity can be determined by Gong et al. 2014.

$$V_N(r_0) = \frac{(1-k)}{\left[1 - k.\exp\left(-\frac{2\,\gamma_{LC}\,cos\theta}{r_0 - \delta}\,\frac{\nu_L}{RT}\right)\right]} \times \frac{[1+(c-1)k]\exp\left(-\frac{2\,\gamma_{LC}\,cos\theta}{r_0 - \delta}\,\frac{\nu_L}{RT}\right)}{\left[1 - (c-1)k.\exp\left(-\frac{2\,\gamma_{LC}\,cos\theta}{r_0 - \delta}\,\frac{\nu_L}{RT}\right)\right]} \quad (13)$$

where:

$k = \frac{\left(1 - \frac{1}{n}\right)C - 1}{C - 1}$

$n = \left(2.5 + \frac{15}{t}\right)\left(0.33 + 2.2\frac{w}{c}\right) \times 1.5$

$C = \exp\left(\frac{855}{T}\right)$

k, C are coefficients of the BSB model, and they depend on the age of concrete, the temperature and the water/cement ratio

γ_{LC} is the liquid–crystal interface energy

δ is the thickness of the liquid-like-layer

θ is the liquid water angle

ν_L is the molar volume

$\frac{w}{c}$ is the water cement ratio

t is the time

The normalized cumulated pore volume depends on the radius and the temperature but in this case the temperature is considered constant.

For all pore radius higher than r_0 we have:

$$V_N(r \geq r_0) = 1 - V_N(r_0) \quad (14)$$

Then, the pore size distribution can be defined as:

$$\varphi(r_0) = \frac{d\,V_N(r \geq r_0)}{dr} \quad (15)$$

For cement paste, the amount of mesopores and

macropores can be neglected.

pores (<100nm) at the level of C-S-H.

$$V_N(r) = \frac{d\,W_N(r)}{dr} = \frac{(1-k)[1+(C-1)k]exp\left(-\frac{2\,\gamma_{LC}\,cos\theta}{(r-\delta)RT}\upsilon_l\right).\left[1+(C-1)k^2\,exp\left(-\frac{4\,\gamma_{LC}\,cos\theta}{(r-\delta)RT}\upsilon_l\right)\right]}{\left\{\left(1-k\,exp\left(-\frac{2\,\gamma_{LC}\,cos\theta}{(r-\delta)RT}\upsilon_l\right)\left[1+(C-1)k\,exp\left(-\frac{2\,\gamma_{LC}\,cos\theta}{(r-\delta)RT}\upsilon_l\right)\right]\right)\right\}^2}.\frac{2\gamma cos\theta}{(r-\delta)^2RT}\upsilon_l \quad (16)$$

3.2 Saturation of liquid as function of pore radius

Assuming the curvature radius of the crystal is $\boldsymbol{r_c}$, then the volume fraction occupied by pores having a pore entry radius higher than $\boldsymbol{r_c}$ can be given as:

$$V_N(r_c) = \int_{r_c}^{r_{max}} \varphi(r)dr \quad (17)$$

The saturation of the liquid is defined as:

$$S_L(r_c) = \frac{V_L}{V_{ett}+V_L} = 1 - S_{ett}(r_c) = 1 - V_N(r_c) \quad (18)$$

The local equilibrium at the interface of crystal obeys the Laplace-Young equation. Rhardane et al. [9] gives relation between the crystallization pressure and the radius of pore in the case of freeze thaw behaviour of cementitious materials, which can be reformulated for ettringite crystallization as follows:

$$P_c - P_l = \frac{RT}{\bar{V}_{crys}} \ln\left(\frac{Q_{reac}}{K_{reac}}\right) = \frac{\gamma_{LC}}{r_H} \quad (19)$$

$$r_H = \lambda(r-\delta) \quad (20)$$

where:
r_H is the hydraulic radius of the interface
$\bar{V}_{crys}$ is the molar volume of crystal (ettringite in our case)
λ is the shape factor (equal to 0.5 for hemispherical ice front, and 1 for a spherical one.
From the equation 19 we say that there is an inverse relationship between the crystallization pressure and the radius of pore, that proved the theory of ettringite precipitation in the small

3.3 The saturation and pressure as function of time

Based on the work of Rhardane et al. [9], a new system of equation can be developed to describe the formation of ettringite depending upon the pore saturation, crystallisation pressure and pore wall deformation. The relation of pore saturation becomes:

$$S^{n+1} = \frac{V_L^{n+1}+V_{ett}^{n+1}}{V_p^{n+1}} = \frac{V_m^{n+1}}{V_p^{n+1}} = \frac{V_m^n+\delta V_m^{n+1}}{V_p^n+\delta V_p^{n+1}} \quad (21)$$

where:

$$V_m = V_L + V_{ett} \quad (22)$$

δV_m^{n+1} corresponds to the change in volume occupied by solid-liquid mixture of water and ettringite and δV_P^{n+1} represents change pore volume between instants t^n and t^{n+1}. The question now is to determine δV_m^{n+1} that quantify the variation of volume of ettringite between t^n and t^{n+1}. Considering ettringite precipitation as the main source of volume change, we can write the following equation:

$$\delta V_m^{n+1} = V_m^n \times \frac{\Delta V_{ett}^{n+1}}{V_L^0+V_{ett}^n} = V_m^n \times (S_{ett}^{n+1} - S_{ett}^n) \quad (23)$$

The change in the volume of the pore can be calculated from the strain tensor.

So, we obtain the following incremental expression of the virtual degree of saturation at t^{n+1} as a function of volume expansion caused by ettringite formation, the change in pore volume at t^n:

$$S^{n+1} = S^n[1 + (S_{ett}^{n+1} - S_{ett}^n)] \times \left[1 + \frac{tr(\epsilon_p^{n+1} - \epsilon_p^n)}{1 + tr(\epsilon_p^n)}\right]^{-1} \quad (24)$$

If $S^{n+1} > 1$, the expansive (negative) pressure p_P^{n+1} acting on the pore walls becomes:

$$\sigma_p^{n+1} = -p_P^{n+1} I \quad (25)$$

and the corresponding strain at t^{n+1} can be calculated as:

$$\epsilon_p^{n+1} = -\left[\frac{1+v}{E} P_p^{n+1} I - \frac{v}{E} tr(P_p^{n+1} I) I\right] \quad (26)$$

Therefore, the incremental expression of the pressure induced by ettringite precipitation in the pore can be given as:

$$P_p^{n+1} = P_p^n \times (S_{ett}^{n+1} - S_{ett}^n) - (S_{ett}^{n+1} - S_{ett}^n) \times K_{hom}^{n+1} \quad (27)$$

where:
K_{hom} is the equivalent bulk modulus which depends on the properties of the water and ettringite phases.

$$K_{hom}^{n+1} = (S_L K_L^{-1} + S_{ett} K_{ett}^{-1})^{-1} \quad (28)$$

3.4 The variation of ettringite saturation in time

From the kinetic law defined previously for the kinetic rate of ettringite formation, we can write in terms of saturation:

$$\frac{dS_n}{dt} = \pm k_n A_{mn,s} M_n \beta_n |1 - \Omega_n| \quad (29)$$

$$\frac{S_{ett}^{n+1} - S_{ett}^n}{t^{n+1} - t^n} = \pm k_{ett} A_{ett,s} M_{ett} \beta_{ett} |1 - \Omega_{ett}| \quad (30)$$

β_{ett} is the ratio between mass of water and the mass of ettringite = 0.01435
Thus, the final system to solve is the following:

$$S^{n+1} = S^n\left[1 + k_{ett} A_{ett,s} M_{ett} \beta_{ett} (1 - \Omega_{ett}) \Delta t\right] \times \left[1 + \frac{tr(\epsilon_p^{n+1} - \epsilon_p^n)}{1 + tr(\epsilon_p^n)}\right]^{-1} \quad (31)$$

$$P_p^{n+1} = P_p^n \times \left(k_{ett} A_{ett,s} M_{ett} \beta_{ett} (1 - \Omega_{ett}) \Delta t\right) - \left(k_{ett} A_{ett,s} M_{ett} \beta_{ett} (1 - \Omega_{ett}) \Delta t\right) \times K_{hom}^{n+1} \quad (32)$$

$$\epsilon_p^{n+1} = -\left[\frac{1+v}{E} P_p^{n+1} I - \frac{v}{E} tr(P_p^{n+1} I) I\right] \quad (33)$$

where:
Ω_{ett} is the saturation index of ettringite; v is the Poisson ratio; E is the Young modulus (GPa); K_{ett} is the rate constant (moles per unit mineral surface area per unit time); $A_{ett,s}$ is the specific reactive (surface area per kg H_2O); K_{hom} is the equivalent bulk modulus of the liquid–solid water mixture (GPa).
The schematic representation of the chemo-mechanical modelling approach for sulfate attack is presentation in Figure 2.

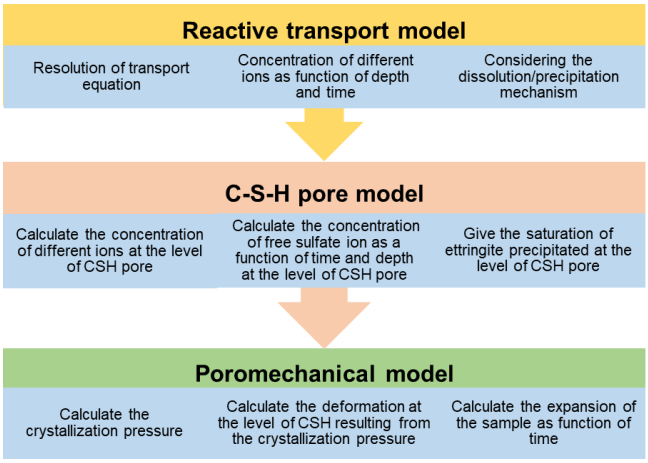

Figure 2: Schematic representation of chemo-mechanical modelling of sulfate attack.

4 RESULTS AND DISCUSSION

4.1 Validation of C-S-H pore model

In the first step to validate the chemical kinetics, the experimental results of Soive et al. [11] was used. In this study, two cement paste cylindrical specimens with 160 mm of height and 20 mm in diameter were exposed to 3 g/l of Na_2SO_4 solution for at least 160 days. Cement used was CEMI 52.5N CE CP2 NF, with a water/cement ratio of 0.4. The specimens were coated on their both ends with a water-proof vinylester resin, thus exposed to sulfate attack only on their circumferential surfaces at a

controlled value pH of 7.5. For the transport data the effective diffusion coefficient D_e of species j in cement paste was considered as a function of tortuosity τ, porosity ϕ, and pure diffusion coefficient $D_{j,w}$ of species j in water. The product between tortuosity τ and porosity ϕ was assumed to be constant, in addition the effective diffusion coefficient is chosen equal to 3.4×10^{-12} m^2/sec for the present hydrated cement paste thus the product between tortuosity and porosity equal to 1.99×10^{-3}. This effective diffusion coefficient value is supposed to be the same for all species in cement paste. More details on the properties and composition can be found in Soive et al. [8].

The proposed numerical model allows computing the percentage of sulfate ions in the pore solution, on to the C-S-H surface or in the solid species, as a function of depth and time output as shown in Figure 3. The amount of free sulfate ions present in the pore solution occupies the smallest quantity of all the contributions. However, the behaviour of the total amount of sulfate ions depends greatly on the amount of sulfate ions adsorbed on C-S-H surface and sulfate ions precipitated. Therefore, it approves the importance to investigate the mineral dissolution/precipitation (such as monosulfoaluminate, ettringite…) and the physicochemical interactions between sulfate ions and solid species in order to understand their influence. The comparison of result given by the numerical model is very close to the experimental results. The C-S-H pore model is able to produce local information since we focalize at the level of C-S-H, whereas; there is lack of experimental results at this level in the literature due to difficult experimental protocols.

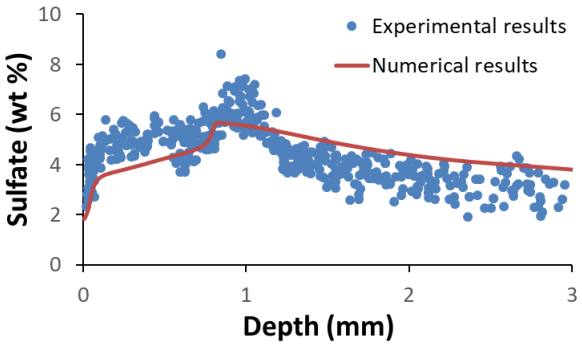

Figure 3: Comparison between experimental results Soive et al. [11], the numerical results of C-S-H pore model results.

4.2 Validation of poromechanical model

In this next step, the results of C-S-H pore model and especially the concentration of sulfate ions have been used in the poromechanical model and comparison is performed with experimental results from the literature. For this purpose, the experimental study of Massaad et al. 2016 [12] was used. In this study, tests were performed on mortar cylindrical samples of 160 mm of height and 20 mm in diameter. Mortar samples were kept in mould for 48h then in saturated limewater for 26 days before exposure to sulfate attack. The laboratory procedure consisted in immersing the mortar samples in a 3 g/l of Na_2SO_4 solution at controlled constant temperature (20°C) and pH (7.5). Although three different types of cement with different chemical composition were used, only the cement CEMI SR 5 PM was used in this study. For the transport problem, same diffusion coefficient of the previous simulation was used.

The C-S-H pore model shows that concentration of sulfate ions in the pore of C-S-H is higher for small depths (0 to 2 mm) as shown in Figure 4 but after this depth, it becomes almost zero, this is due to the complexation on the surface of C-S-H. In fact, if we see the Figure 5, the concentration of sulfate ions adsorbed on the C-S-H surface becomes more important in the range (0.5 mm to 5 mm) and it approaches to zero at the depth of 6 mm, which is why there is no precipitation of ettringite in this range of depth as we see in the Figure 6. The concentration of sulfate ions in the pore becomes higher (Figure 4) when the

desorption of sulfate ions begins (depth > 6 mm) that will lead to precipitation of ettringite as it is shown in the Figure 6.

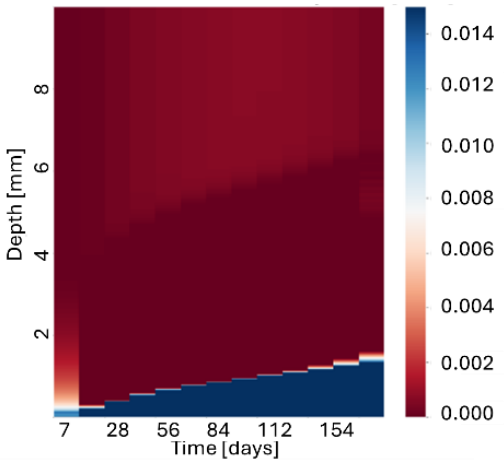

Figure 4: Concentration total of sulfate ions in the C-S-H pore (mol/l).

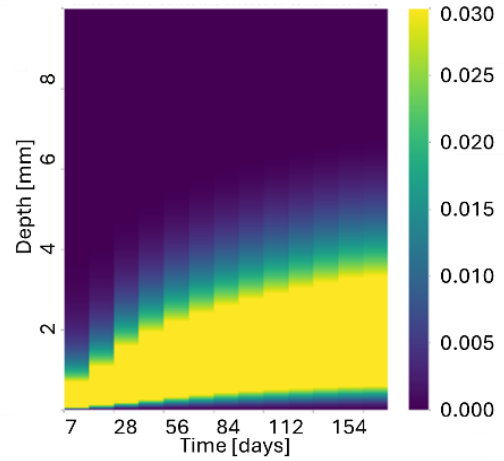

Figure 5: Concentration of sulfate ions adsorbed on C-S-H (mol/l).

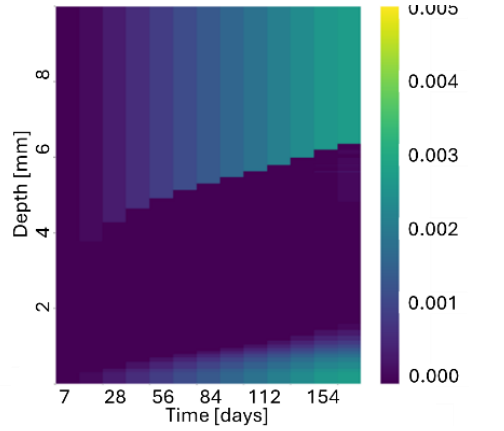

Figure 6: Concentration of sulfate ions precipitated as ettringite in the gel pore (mol/l)

The poromechanical model allows us to calculate the pressure and strain as a function of depth and time output. The strain at C-S-H level has the same evolution curve as the sulfate ion concentration in the pore of C-S-H. In fact, if we see the strain at 160 days of exposure, the strain is more important in smaller depths (0 to 2 mm) and then the deformation is almost zero and then begins to increase after a depth of 6 mm as shown in the Figure 7. As a first estimation of expansion, the maximum strain (mm/m) over all depths is calculated at every time output to compare it with the expansion of specimens experimentally observed as shown in the Figure 8. The result of the numerical model is very close of the experimental results of expansion, that validate the proposed numerical model. Thus, it strengthen our assumption of expansion mechanism of ESA that the expansion begins at the level of C-S-H when the two conditions are available: the pores at the level of C-S-H provide the crystal a supersaturated solution where it can grow, which further provides the energy for expansion and causes crystallization pressure. The crystal grows in a confined space and exert the expansive force on the walls of the pore.

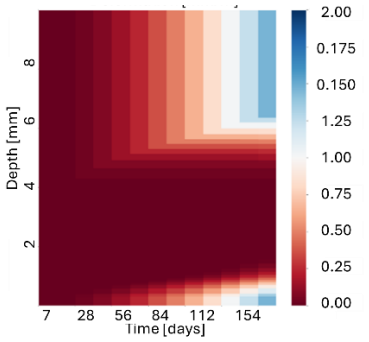

Figure 7: Strain at the level of C-S-H (mm/m).

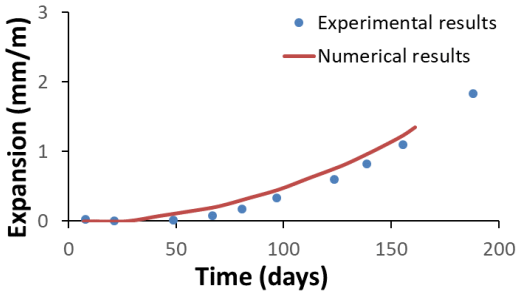

Figure 8: Expansion in (mm/m), comparison between

experimental and numerical results

5 CONCLUSIONS

The main advantages of numerical modelling and simulation is that they require significantly less time and resources than experimental testing. Thus, they can be used to understand underlying mechanisms. The proposed chemo-mechanical numerical model gives good results comparable to the experimental results along with visualization and quantification of the effect of different mechanisms of external sulfate attack in the material and locally at the level of C-S-H phase.

From the comparison of expansion due to the deformation in the level of C-S-H and the expansion observed experimentally, especially in the first's days of exposure where expansion is due to elastic deformation without cracks, we concludes that the expansion begins at the level of C-S-H phase, which is the perfect environment where the crystal grows in a confined space and provide an important energy of expansion.

REFERENCES

[1] R. Tixier and B. Mobasher, "Modeling of Damage in Cement-Based Materials Subjected to External Sulfate Attack. I: Formulation," *J. Mater. Civ. Eng.*, vol. 15, no. 4, pp. 305–313.

[2] M. Basista and W. Weglewski, "Micromechanical modelling of sulphate corrosion in concrete: influence of ettringite forming reaction," *Appl. Mech*, vol. 35, no. 3, pp. 29–52, 2008.

[3] B. Bary, "Simplified coupled chemo-mechanical modeling of cement pastes behavior subjected to combined leaching and external sulfate attack," *Int. J. Numer. Anal. Methods Geomech.*, vol. 32, no. 14, pp. 1791–1816.

[4] B. Bary, N. Leterrier, E. Deville, and P. Le Bescop, "Coupled chemo-transport-mechanical modelling and numerical simulation of external sulfate attack in mortar," *Cem. Concr. Compos.*, vol. 49, pp. 70–83.

[5] T. Schmidt, B. Lothenbach, M. Romer, J. Neuenschwander, and K. Scrivener, "Physical and microstructural aspects of sulfate attack on ordinary and limestone blended Portland cements," *Cem. Concr. Res.*, vol. 39, no. 12, pp. 1111–1121.

[6] C. Yu, W. Sun, and K. Scrivener, "Mechanism of expansion of mortars immersed in sodium sulfate solutions," *Cem. Concr. Res.*, vol. 43, no. 1, pp. 105–111.

[7] Y. Gu, P. Dangla, R. P. Martin, O. Omikrine Metalssi, and T. Fen-Chong, "Modeling the sulfate attack induced expansion of cementitious materials based on interface-controlled crystal growth mechanisms," *Cem. Concr. Res.*, vol. 152, p. 106676.

[8] A. Soive and V. Q. Tran, "External sulfate attack of cementitious materials: New insights gained through numerical modeling including dissolution/precipitation kinetics and surface complexation," *Cem. Concr. Compos.*, vol. 83, pp. 263–272.

[9] A. Rhardane, S. Al Haj Sleiman, S. Y. Alam, and F. Grondin, "A quantitative assessment of the parameters involved in the freeze–thaw damage of cement-based materials through numerical modelling," *Constr. Build. Mater.*, vol. 272, p. 121838.

[10] B. Lothenbach and F. Winnefeld, "Thermodynamic modelling of the hydration of Portland cement," *Cem. Concr. Res.*, vol. 36, no. 2, pp. 209–226.

[11] A. Soive, E. Roziere, and A. Loukili, "Parametrical study of the cementitious materials degradation under external sulfate attack through numerical modeling," *Constr. Build. Mater.*, vol. 112, pp. 267–275.

[12] G. Massaad, E. Rozière, A. Loukili, and L. Izoret, "Advanced testing and performance specifications for the cementitious materials under external sulfate attacks," *Constr. Build. Mater.*, vol. 127, pp. 918–931.